International Journal of Precision Engineering and Manufacturing Vol. 6, No.1, January 2005.

Force Prediction and Stress Analysis of a Twist Drill from Tool Geometry and Cutting Conditions

Kug Weon Kim[1,#] and Tae-Kil Ahn[2]

[1] Department of Mechanical Engineering, Soonchunhyang University, Asan, Chungnam, South Korea
[2] Department of Mechanical Engineering, Hoseo University, Asan, Chungnam, South Korea

ABSTRACT

Drilling process is one of the most common, yet complex operations among manufacturing processes. The performance of a drill is largely dependent upon drilling forces. Many researches focused on the effects of drill parameters on drilling forces. In this paper, an effective theoretical model to predict thrust and torque in drilling is presented. Also, with the predicted forces, the stress analysis of the drill tool is performed by the finite element method. The model uses the oblique cutting model for the cutting lips and the orthogonal cutting model for the chisel edge. Thrust and torque are calculated analytically without resorting to any drilling experiment, only by tool geometry, cutting conditions and material properties. The stress analysis is performed by the commercial FEM program ANSYS. The geometric modeling and the mesh generation of a twist drill are performed automatically. From the study, the effects of the variation of the geometric features of the drill and of the cutting conditions of the drilling on the drilling forces and the stress distributions in the tool are calculated analytically, which can be applicable for designing optimal drill geometry and for improving the drilling process.

Key Words : Stress analysis, Twist drill, Finite element method, Tool geometry, Cutting conditions

1. Introduction

Drilling process is one of the most common, yet complex operations among manufacturing processes. Recently the need for precise and efficient drilling process is increasing in the whole industry, especially in electronic industry. The trend towards higher density printed circuit boards (PCB) requires smaller holes down to 0.1 mm diameter to be drilled through the board layers. As the diameter of the hole drilled is smaller, the cost for the hole drilled is exponentially increasing. Accordingly it is very important to select an appropriate drill tool and drilling conditions.

Manuscript received: February 23, 2004 ;
Accepted: October 11, 2004
Corresponding Author:
Email: kimkug1@sch.ac.kr
Tel: +82-41-530-1225, Fax: +82-41-530-1550

Drill performance is closely related to the drilling force. Many researches for the effect of drill geometry and cutting conditions on drilling forces have been performed [1]. Some researches include the prediction of drill tool deformation by finite element method [2], where drill geometry was modeled in 3-dimentional configuration but only feed rate and work material hardness were considered. Hinds et al. [3] obtained the measured forces from experimental tests and, with using those as loading conditions, analyzed the stress distribution of micro-drills. Some focused on searching the geometry parameter reducing the drilling forces with analyzing the relation between drill geometry and drilling force. However, drill performance can be enhanced when both the stresses and deformations of a drill tool should be considered.

In this paper, first, an effective model to predict thrust and torque analytically in drilling is presented. The method is to determine the continuous distributions of

thrust and torque along the cutting lips and the chisel edge. The oblique cutting model and the orthogonal cutting model are used for the cutting lips and the chisel edge respectively. Secondly, the stress distributions in the drill tool with the analytically calculated drilling forces from the tool geometry and cutting conditions are analyzed by finite element method. Drill geometry is automatically modeled and meshed with the information of geometry parameters with the aid of ANSYS program.

2. Prediction of Drilling Forces

Many researchers proposed various models to calculate thrust and torque during drilling [4-6]. Some of these models are purely empirical and hold only for a specific situation, while others are more general-purpose models. Few theoretical and predictable works have been undertaken on drilling. A prediction model for drilling forces requires no preliminary experimental results.

The drill point is defined by geometrical parameters that depend on the cutting geometry of the two active parts, the cutting lips and the chisel edge as shown in Fig. 1.

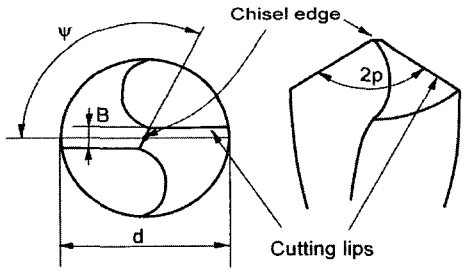

Fig. 1 Configuration of drill point

Cutting lips

Since the drilling process can be represented as an oblique cutting process which has changing inclination angles depending upon the relative radial position of the cutting edge, each element of the cutting edge can be considered to be analogous to an oblique single point tool as shown in Fig. 2(a) with a rake angle equal to the dynamic rake angle α_D, which comprises the effects of feed rates.

In a shear plane model of the orthogonal cutting process in Fig. 2(b), the shear angle can be estimated from the Merchant equation as

$$\phi = \frac{\pi}{4} + \frac{\alpha_D - \lambda}{2} \tag{1}$$

Here, the friction angle could be assumed independent of cutting speed [7].

$$\lambda = \frac{\pi}{6} + \frac{\alpha_D}{2} \tag{2}$$

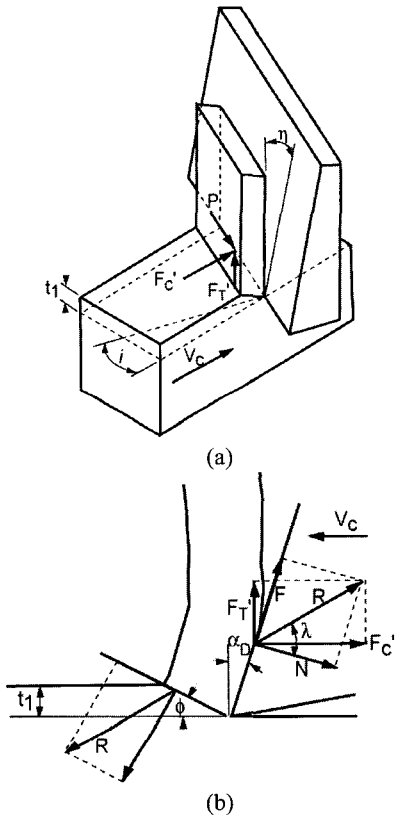

Fig. 2 Shear plane model: (a)oblique; (b)orthogonal

Inclination angle i and dynamic rake angle α_D at cutting point M are given by the following equations:

$$i = \sin^{-1}(\sin\omega \cdot \sin p) \tag{3}$$

$$\alpha_D = \alpha_S + \beta \tag{4}$$

where p is the half point angle of the tool, α_S is the normal rake angle and β is the feed angle. ω is the

intermediate angle as presented on Fig. 3 and is calculated from the geometrical parameters of the drill by:

$$\omega = \sin^{-1}(B/2r) \tag{5}$$

and

$$\alpha_S = \tan^{-1}\left(\frac{\tan\delta\cdot\cos\omega}{\sin p - \cos p\cdot\tan\delta\cdot\sin\omega}\right) \tag{6}$$

$$\beta = \tan^{-1}\left(\frac{f\cdot\sin p}{2\pi r\cdot\cos\omega}\right) \tag{7}$$

where B is the web thickness, r is the distance from the drill axis to the point M, f is the feed rate and δ is the helix angle at point M, given by:

$$\delta = \tan^{-1}\left(\frac{2r}{d}\tan\delta_0\right) \tag{8}$$

and δ_0 is the helix angle at the periphery of the tool.

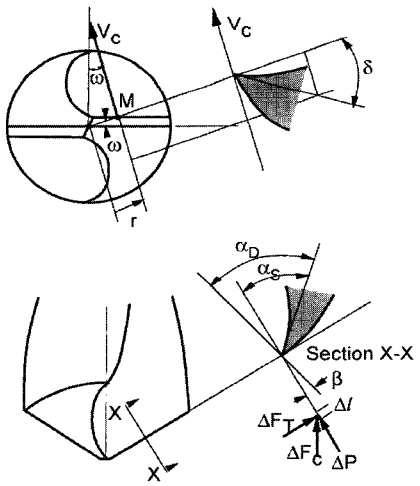

Fig. 3 Dynamic geometry of cutting edge

Therefore, for a given speed and feed rate, above equations determine the shear angle.

The forces F_C' and F_T' in Fig. 2 indicate the forces in the direction of and normal to the cutting velocity, Vc with the oblique angle i. The forces ΔF_C and ΔF_T in Fig. 3 are the forces for each sliced element of main cutting lips that are generated by rotating F_C' and F_T' and by an amount of the feed angle β. The force ΔP is normal to ΔF_C and ΔF_T. Therefore, the forces can be found by adding the feed angle to the available model [8].

$$\Delta F_C = \frac{t_1\cdot\Delta l\cdot k_S\cos(\lambda-\alpha_D+\beta)}{\sin\phi\cdot\cos(\phi+\lambda-\alpha_D)} \tag{9}$$

$$\Delta F_T = \frac{t_1\cdot\Delta l\cdot k_S\sin(\lambda-\alpha_D+\beta)}{\sin\phi\cdot\cos(\phi+\lambda-\alpha_D)} \tag{10}$$

$$\Delta P = \sqrt{\Delta F_C^2+\Delta F_T^2}\sin\lambda\cdot\tan\eta \tag{11}$$

where : $t_1 = \dfrac{f\cdot\sin p\cdot\cos\beta}{2}$

Δl : length of sliced element

k_S : shear strength of the work material

η (chip flow angle) $= \tan^{-1}(\tan i\cdot\cos\alpha_D)$

Chisel edge

In a standard twist drill, the chisel edge is perpendicular to the axis of the drill so that the cutting speed is perpendicular to the cutting edge at any point. Previous work [9] on drilling has shown that the cutting phenomenon only acted on a part of the chisel edge, while on another, situated closer to the axis of the tool, an indentation phenomenon occurs. In the cutting part, the method adopted is the orthogonal cutting model with a negative rake angle. The contribution in thrust and in torque of the other part is assumed to be negligible.

The orthogonal cutting model is applied on the part of the chisel edge defined by a dynamic positive clearance angle. The dynamic rake angle α_{DC} and the dynamic clearance angle ν_{DC} as shown in Fig. 4 are given by

$$\alpha_{DC} = \beta_C - \alpha_{SC} \tag{12}$$

$$\nu_{DC} = (\pi/2-\alpha_{SC})-\gamma_f \tag{13}$$

where : $\alpha_{SC} = \tan^{-1}(\tan p\cdot\sin\psi)$

$\beta_C = \tan^{-1}(f/2\pi r)$

ψ : chisel edge angle as shown in Fig. 1

The above equations show that as the radius r decreases, β_C increases and ν_{DC} decreases and the radius r_C, at which $\nu_{DC} = 0$, is found as

$$r_C = \frac{f\cdot\tan p\cdot\sin\psi}{2\pi} \tag{14}$$

For the case of high negative rake angle as shown in Fig. 5, the shear angle and friction angle could be assumed as [10]

$$\phi_C = \pi/2 + 1.2(\alpha_{DC} - \lambda_C) \tag{15}$$

$$\lambda_C = \pi/4 + 2\alpha_{DC}/3 \tag{16}$$

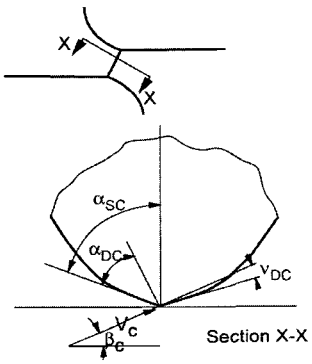

Fig. 4 Dynamic geometry of chisel edge

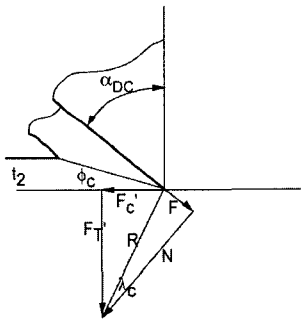

Fig. 5 Shear plane model with negative rake angle

The forces F_C' and F_T' in Fig. 5 are the forces in the direction of and normal to the cutting velocity, Vc. The forces ΔF_{CC} and ΔF_{TC} for each element (Δr) generated by rotating F_C' and F_T' by an angle β_C, are found as

$$\Delta F_{CC} = \frac{t_2 \cdot \Delta r \cdot k_S \cos(\lambda_C - \alpha_{DC} + \beta)}{\sin\phi_C \cdot \cos(\phi_C + \lambda_C - \alpha_{DC})} \tag{17}$$

$$\Delta F_{TC} = \frac{t_2 \cdot \Delta r \cdot k_S \sin(\lambda_C - \alpha_{DC} + \beta)}{\sin\phi_C \cdot \cos(\phi_C + \lambda_C - \alpha_{DC})} \tag{18}$$

where : $t_2 = \dfrac{f \cdot \cos\beta}{2}$

Thrust and torque prediction

The thrust (TH_L) and torque (TO_L) developed in the main cutting lips are found by integrating the force components of each element of the cutting lips.

$$TH_L = 2\left(\int_{d'/2}^{d/2} \sin\, pdF_T + \int_{d'/2}^{d/2} \cos\, pdP\right) \tag{19}$$

$$TO_L = 2\left(\int_{d'/2}^{d/2} r\cos i dF_C + \int_{d'/2}^{d/2} r\sin i \sin\, pdP\right) \tag{20}$$

Integrating ΔF_{CC} and ΔF_{TC} along the radius of the drill on the negative rake angle region, we obtain the following equations for the drilling thrust (TH_C) and torque (TO_C) on the chisel edge.

$$TH_C = 2\int_{r_c}^{d'/2} dF_{TC} \tag{21}$$

$$TO_C = 2\int_{r_c}^{d'/2} dF_{CC} \tag{22}$$

The total thrust (TH) and torque (TO) can be predicted by adding the force components from the cutting lips and the chisel edge, that is:

$$TH = TH_L + TH_C \tag{23}$$

$$TO = TO_L + TO_C \tag{24}$$

The above equations are functions of drill tool geometry, drilling conditions and the shear strength of work material. Among these, the shear strength is the only unknown.

Shear strength of material at the shear plane is another challenge in calculating drilling forces since it greatly changes depending on strain, strain rate, temperature and cutting condition, etc. Ignoring the effects mentioned above, and assuming that tensile and shear strength of the material have same strain hardening behavior,

$$k_S \approx \tau_U : \frac{\tau_U}{\tau_y} = \frac{\sigma_U}{\sigma_Y} \tag{25}$$

where σ_Y and σ_U are tensile yield and ultimate strength, respectively, and τ_Y and τ_U are shear yield and ultimate strength of material. From the octahedral shear stress relation,

$$\tau_y = \frac{\sqrt{2}}{3}\sigma_y \qquad (26)$$

Now, we can predict the drilling forces - thrust and torque - from the drill tool geometry and drilling conditions without any preliminary experimental results. Fig. 6 shows the flow chart of thrust and torque computation.

Fig. 7 shows the measured data [4] and the predicted thrust and torque for Aluminum 2024 material. The solid lines are calculated results and the circle symbols are measured data. The drill tool geometry and cutting conditions are as follows:

- Drill diameter: 9.50mm, 6.35mm
- Point angle: 118°
- Chisel edge angle: 55°
- Web thickness: 1.40mm, 0.94mm
- Rotational speed: 285rpm
- Various feed rates

The calculated results show good correlation with experimental data.

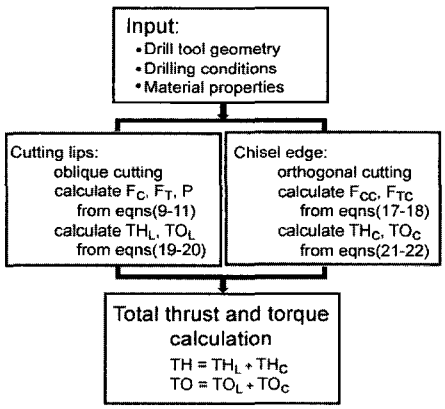

Fig. 6 Flow chart of thrust and torque computation

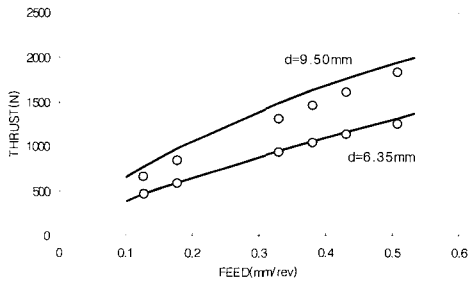

(a)

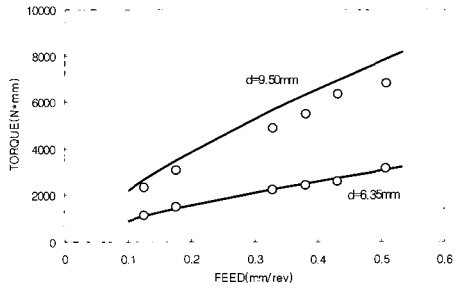

(b)

Fig. 7 Measured(circle symbol) and calculated(solid line) thrust and torque of drill(speed=285rpm): (a) thrust; (b) torque

3. Geometry Modeling

Fig. 8 shows the co-ordinates at the drill point for a twist drill. The surface containing these points is referred to as the zero surface. The equations required to calculate each of the co-ordinate points 1~8 are shown in Table 1.

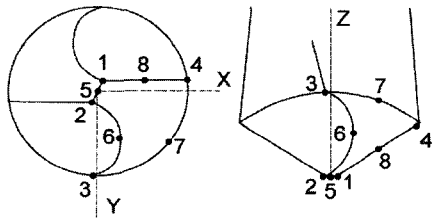

Fig. 8 Nodal points on the twist drill

Table 1 Coordinates of nodal point

Nodal point	Coordinates		
	X	Y	Z
1	0.5B/tanψ	-0.5B	0
2	-0.5B/tanψ	0.5B	0
3	$0.5d\cos\theta'_2$	$0.5d\sin\theta'_2$	z_{04} +$(\theta_L/360)\pi d\tan\nu$
4	$0.5(d^2-B^2)^{1/2}$	-0.5B	0.5 (d-B/tanψ)/tan$p$
5	0	0	0
6	$0.5(x_{03}-x_{02})$	d/2 +$0.5(y_{03}-y_{02})$	$0.5z_{03}$
7	0.5d $\cos(\theta_L/2)$	0.5d $\sin(\theta_L/2)$	z_{04} +$(\theta_L/720)\pi d\tan\nu$
8	$0.5(x_{01}-x_{04})$	-0.5d	$0.5\ z_{04}$

where ν: clearance angle

θ_L: land angle = 180/(1+F)

F: flute/land ratio

$\theta'_2 = \theta_L - \theta'_1$

$\theta'_1 = \tan^{-1}(y_{04}/x_{04})$

As one moves along the axis of the drill away from the drill point, the section rotates. The angle of rotation is related to the distance of the section from the drill point and the helix angle of the drill. The co-ordinates of a surface, helically parallel to the zero surface, define a s-surface. This is placed at a distance S from the zero surface along the z-axis. The series of equations required to calculate subsequent s-surfaces are as follows:

$$\theta = 2\pi S/L \text{ radians for } S \leq L \quad (27)$$

$$\theta = 2\pi \times \text{fractional part of } (S/L) \text{ radians for } S > L \quad (28)$$

where L : the lead of helix ($=\pi d/\tan\delta_o$)

δ_o : helix angle

Therefore, the co-ordinates (x, y, z) of the point on the s-surface corresponding to the point (x_0, y_0, z_0) on the zero surface are given by:

$$x = x_0 \cos\theta - y_0 \sin\theta \quad (29)$$

$$y = x_0 \sin\theta + y_0 \cos\theta \quad (30)$$

$$z = z_0 + S \quad (31)$$

Also, the symmetrically placed elements in the third quadrant (x', y', z') are:

$$x' = -x, \; y' = -y, \; z' = z \quad (32)$$

From the equations, drill geometry can be determined. A geometric modeling for a twist drill is performed by APDL, the programming language of commercial FEM program ANSYS. Fig. 9 shows the flow chart of drill geometry modeling, 3-dimentional drill geometry modeled and the finite element model.

According to co-ordinate system as shown in Fig. 8, cutting force components in the direction of 3 axes are obtained as follows:

at cutting lips region

$$\Delta F_{xL} = \Delta F_T \cos p + \Delta F_C \cos i \quad (33)$$

$$\Delta F_{yL} = \Delta F_C \cos i + P \sin i \sin p \quad (34)$$

$$\Delta F_{zL} = \Delta F_T \sin p + P \cos p \quad (35)$$

at chisel edge region

$$\Delta F_{xC} = \Delta F_{CC} \sin\psi \quad (36)$$

$$\Delta F_{yC} = \Delta F_{CC} \cos\psi \quad (37)$$

$$\Delta F_{zC} = \Delta F_{TC} \quad (38)$$

Cutting force components, Fx, Fy and Fz are calculated by integrating the force components of each element of cutting lips and chisel edge, Eqs. (33)-(38).

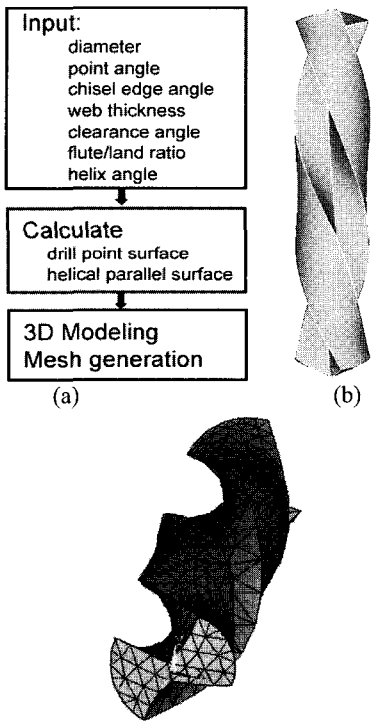

Fig. 9 Automated 3D modeling and mesh generation: (a) drill modeling flow chart; (b) geometric modeling; (c) mesh generation

4. Results and Discussions

For finite element analysis, the opposite end of drill point is fixed, which gives the effect of the drill being

clamped in the spindle collet. Cutting force components in the direction of 3 axes at cutting lips and chisel edge previously mentioned are applied as loading conditions.

As the material property of the drill tool is very brittle, the distributions of principal stress are examined in priority. Fig. 10 shows the distributions of principal stress of the drill tool. The maximum principal stress is located below the lip region and the minimum principal stress is located near to lip region and chisel edge. That is, the failure possibility exists because of tension stress below the lip region and compression stress near the lip region and chisel edge

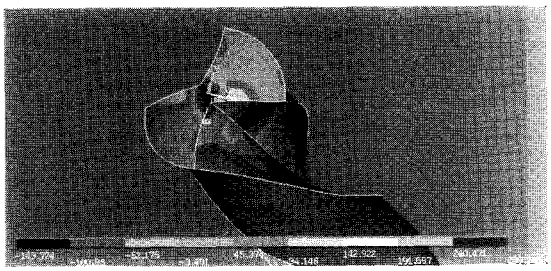

(a)

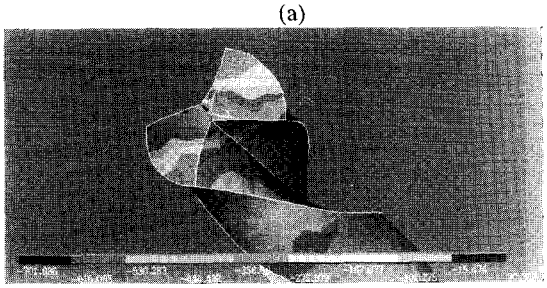

(b)

Fig. 10 Principal stress distribution of the drill: (a) maximum principal stress; (b) minimum principal stress

Drill performance can be examined now by considering together drill force and stress state. As one case to examine the drill performance, the effect of web thickness variation is investigated. Fig. 11 shows the framework of CAD/CAE integration, beginning from drill geometry and drilling conditions to stress analysis.

Fig. 12 shows the variation of cutting force components with the increase of feed and with web thickness variation. For the web thickness variation, x-directional and y-directional cutting forces are little changed over the entire range considered, but z-directional cutting force is largely affected as feed increases. In other words, in case that the feed is relatively large, the decrease of web thickness results in the decrease of z-directional cutting force.

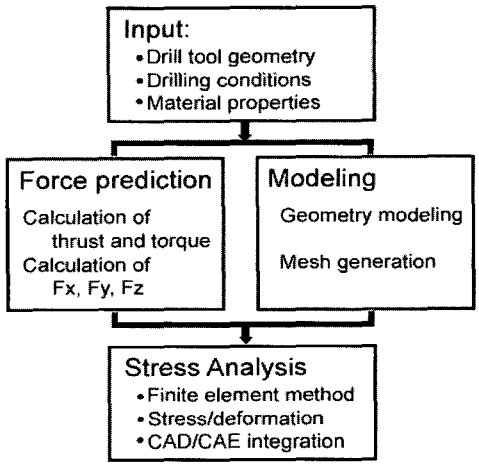

Fig. 11 Framework of CAD/CAE integration

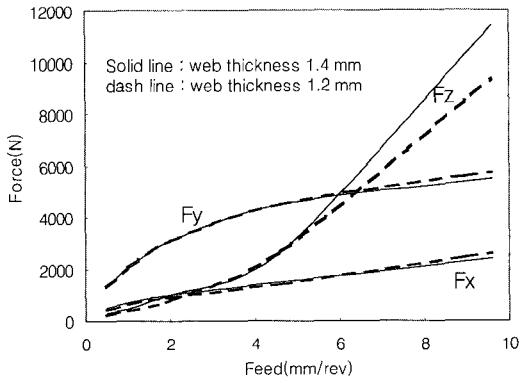

Fig. 12 Drill force with web thickness and feed variations

The cutting force components calculated are then applied as loading conditions and the finite element analysis is performed. Fig. 13 shows the stress distributions of drill point at the condition of 10 mm/rev feed in Fig. 12. At the feed of 10 mm/rev, as z-directional force is largest, the compression stress is occurred at the chisel edge. The drill of 1.2 mm web thickness has smaller z-directional cutting force compared with that of 1.4 mm web thickness but on the contrary has larger minimum principal stress (compression stress), which means that as web thickness decreases, the z-directional cutting force decreases but the compression stress increases.

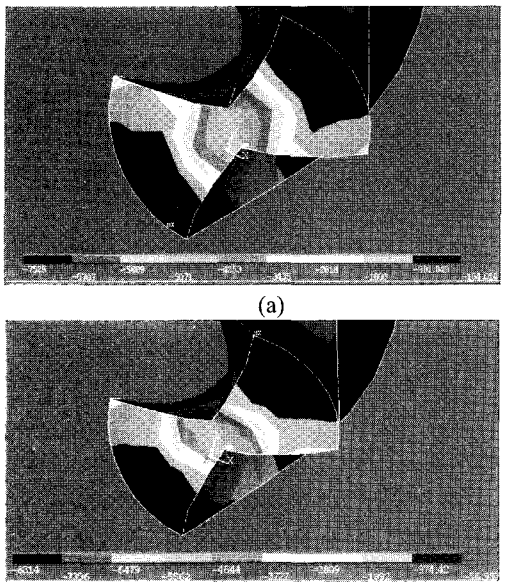

(a)

(b)

Fig. 13 Minimum principal stress distributions: (a) web thickness 1.4mm; (b) web thickness 1.2mm

5. Conclusions

The following conclusions may be drawn from this study:

(1) An effective theoretical model to predict thrust and torque without any experiment in drilling if material properties of work material are in hand is present.

(2) With the aid of cutting force model considering tool geometry and drilling conditions, the effect of drill geometry and cutting conditions on stress distributions and deformation of the drill tool can be analytically predicted.

(3) The effect of web thickness variation on stress state of a drill tool is investigated, which shows the drill of smaller web thickness has smaller z-directional cutting force but may have larger compression stresses compared with that of the larger web thickness.

(4) The analysis procedure performed in this paper can be applicable for designing a new drill tool and selecting drilling conditions toward enhancing drill performance.

Acknowledgement

This work was supported by grant No. (R02-2000-00317) from the Korea Science & Engineering Foundation.

References

1. Kaldor, S. and Lenz, E., "Drill Point Geometry and Optimization," ASME J. Eng. Ind., Vol. 104, pp. 84-90, 1982.
2. Selvam, S. V. M. and Sujatha, C., "Twist drill deformation and optimum drill geometry," Comp. Struct., Vol. 57, pp. 903-914, 1995.
3. Hinds, B. K. and Treanor, G. M., "Analysis of Stress in Micro-Drills Using the Finite Element Method," Int. J. Mach. Tools Manufac., Vol. 40, pp. 1443-1456, 2000.
4. Lee, J. W., Force Analysis of Drill Point Geometry for Optimal Design and Wear Prediction, Ph.D. dissertation, U. of Wisconsin-Madison, 1986.
5. Chandrasekharan, V., Kapoor, S. G., and Devor, R. E., "A Mechanistic Model to Predict the Cutting Force System for Arbitrary Drill Point Geometry," ASME J. Manuf. Sci. Eng., Vol. 120, pp. 563-570, 1998.
6. Rubenstein, C., "The Torque and Thrust Force in Twisting Drilling – I. Theory," Int. J. Mach. Tools Manufac., Vol. 21, pp. 481-489, 1991.
7. William, R. A., "A Study of Drilling Process," ASME, J. Eng. Ind., Vol. 96, pp. 1207-1215, 1974.
8. Lin, C. G.. I. and Oxley, P. L. B., "Mechanics of Oblique Machining: Predicting Chip Geometry and Cutting Forces from Work Material Properties and Cutting Conditions," Proc. Instn. Mech. Engrs., Vol. 186, pp. 66-72, 1972.
9. Armarego, E. J. A. and Cheng, C. Y., "Drilling with Rake Face and Conventional Twist Drills. I: Theoretical Investigation," Int. J. Mach. Tool Des. Res., Vol. 12, p. 17, 1972.
10. Kita, Y. and Ido, M., "A Study of Metal Flow Ahead of Tool Face with Large Negative Rake Angle," ASME, J. Eng. Ind., Vol. 104, pp. 319-325, 1982.